Journal of Molecular Catalysis A: Chemical 350 (2011) 97–102

Contents lists available at SciVerse ScienceDirect

Journal of Molecular Catalysis A: Chemical

journal homepage: www.elsevier.com/locate/molcata

Green catalysts based on bio-inspired polymer coatings and electroless plating of silver nanoparticles

Burcu Çelen[a,b], Dilara Ekiz[b], Erhan Pişkin[a,c], Gökhan Demirel[b,c,*]

[a] Department of Chemical Engineering, Hacettepe University, 06532 Ankara, Turkey
[b] Bio-inspired Materials Research Laboratory (BIMREL), Department of Chemistry, Gazi University, 06500 Ankara, Turkey
[c] Biyomedtek: Center for Bioengineering, 06532 Ankara, Turkey

ARTICLE INFO

Article history:
Received 2 July 2011
Received in revised form
17 September 2011
Accepted 20 September 2011
Available online 28 September 2011

Keywords:
Bio-inspiration
Polydopamine
Catalysis
Nanomaterials
Anodic aluminum oxide (AAO) membranes

ABSTRACT

Herein, a simple but versatile method to develop supported-metal catalysts based on a polydopamine (PDOP) coating and electroless plating of silver nanoparticles (AgNPs) onto nanomaterials (e.g., anodic aluminum oxide (AAO) membranes and polystyrene (PS) nanotubes) for catalytic reduction is demonstrated. The PDOP coating was inspired by the composition of adhesive proteins in mussels. A comparative study on the catalytic activities of the individual AgNPs, AgNPs/PDOP/AAOs with different pore sizes (20–200 nm) and AgNPs/PDOP/PS nanotubes in the reduction of o-nitroaniline (o-NA) to 1,2-benzenediamine (BDA) was carried out. The results indicated that both AgNPs/PDOP/AAO (200 nm) and AgNPs/PDOP/PS exhibited significantly higher catalytic activities than individual AgNPs. We also observed that the PDOP coating alone had the ability to reduce o-NA to BDA. Given their simplicity, efficiency, and flexibility, we believe that these types of green catalysts might find a wide range of applications in organic synthesis and catalysis.

1. Introduction

Supported-metal catalysts, also called "green catalysts", have recently attracted worldwide attention for a variety of applications due not only to their cost effectiveness through catalyst recovery and recycling but also for their removal of toxic metals from the waste stream [1,2]. Therefore, various innovative strategies, including immobilization of the catalysts onto inorganic or organic supports [3,4], liquid/liquid biphasic extractions [5,6], and solvent-free transformations [7,8] have been attempted to develop green catalysts. Although, most supported catalysts have been successfully recycled, the recovered catalysts have some disadvantages, such as lower activities and selectivities, compared to their non-supported analogues. To achieve the desired catalytic activity and selectivity, understanding the interface between the support material and the catalytic moiety, controlling nanoparticle size, shape and density, and tuning of the supports are all important aspects. These problematic variables are quite complex, however, so the design and control of supported-metal catalysts is still a serious challenge in catalysis and materials research.

Nanoparticles, which have catalytic activity, are mostly needed a suitable and stable support to prevent aggregation during the catalytic reaction, and also to provide reusabilty. In recent years, several methods have been reported to immobilize metal nanoparticles on high surface area support materials. The most remarkable techniques for the immobilization of metal particles are direct immobilization onto support and ion exchange [9–12]. Both approaches have some drawbacks. In direct immobilization technique, chemically active supports or extra modification steps are required to immobilize nanoparticles. Moreover, poor immobilized nanoparticle density is another big problem. As for ion exchange technique, certain types of support materials with an ion exchange resin, which mostly consist of a polymeric matrix and a functional group with a mobile ion, is needed to generate metal nanoparticles onto support from a metal precursors in solution phase. Therefore, new techniques, which may provide flexibility in selection of the support materials and high density nanoparticle immobilization or generation, are still crucial.

Recently, Messersmith and co-workers reported a surface modification method [13] using a polydopamine (PDOP) coating based on oxidative polymerization of dopamine in alkaline aqueous media. PDOP coating is a material-independent approach and may be applied to almost any solid surface (e.g., metal oxides, ceramics, and synthetic polymers) on which biomineralization, cell adhesion, wetting control and protein immobilization can occur [14–17].

* Corresponding author at: Bio-inspired Materials Research Laboratory (BIMREL), Department of Chemistry, Gazi University, 06500 Ankara, Turkey.
Tel.: +90 312 2021530; fax: +90 312 2122279.
E-mail address: nanobiotechnology@gmail.com (G. Demirel).

1381-1169/$ – see front matter © 2011 Elsevier B.V. All rights reserved.
doi:10.1016/j.molcata.2011.09.017

This method also serves for in situ growing of metal nanoparticles. Despite the superior properties of PDOP, its use in catalysis applications as a support material remains unexplored.

In this work, a simple and useful strategy is demonstrated for developing supported-metal catalysts based on PDOP coating and electroless plating of silver on nanoporous anodic alumina membranes (AAO) with various pore sizes (20–200 nm) and on polystyrene (PS) nanotubes (Scheme 1a and b). Their catalytic efficiencies in the reduction of o-nitroaniline (o-NA) using sodium borohydride were evaluated. The reduction of o-NA is a model reaction that has been widely used for the quantification and comparison of the catalytic activity of different metal nanoparticles and their immobilized forms.

2. Experimental

2.1. Preparation of AgNPs/PDOP/AAOs and AgNPs/PDOP/PS nanotubes

All the chemicals and solvents were of analytical grade and used without further purification. Deionized water of 18 MΩ cm^{-1} was also used in the experiments and for rinsing. The following protocol was used to prepare AgNPs/PDOP/AAOs: 20 mg of dopamine was first dissolved in 10 mL of Tris–HCl buffer solution (10 mM, pH 8.5), and AAO membranes (Whatman, Inc., USA) having different pore sizes (i.e., 20, 100 and 200 nm) were then immersed in this solution for various time intervals (3–24 h). Afterwards, PDOP-coated membranes were transferred into an $AgNO_3$ solution (50 mM) for 24 h to grow silver nanoparticles (AgNPs).

To prepare AgNPs/PDOP/PS nanotubes, two drops of PS solution (10%, w/w) in toluene were first placed onto the 200 nm pore size AAO membrane. After solvent evaporation, samples were soaked in a phosphoric acid solution (5%, v/v) for 30 min, which resulted in the widening of the nanopores of the AAO. Afterwards, the inner and outer walls of the PS nanotubes were coated with PDOP, and AAO templates were completely etched with a 5% H_3PO_4 and 1% HF solution. AgNPs were formed on the top and sides of the PDOP-coated nanotube as mentioned above.

2.2. Catalytic reduction of o-nitroaniline

A typical catalysis experiment was carried out as follows. A AgNPs solution (1.02 nM) or prepared supported-catalyst was first dispersed in a mixture of 10 mL of deionized water and 10 mL of a freshly prepared $NaBH_4$ solution (1.2 M). The mixture was stirred for 30 min at room temperature. The o-NA solution (10 mL, 3.4×10^{-3}M) was then added to the mixture and stirred at room temperature until the yellow solution became colorless. The catalyst efficiency was monitored by removing aliquots of the reaction mixture at certain time periods and measuring the UV–vis spectra.

3. Results and discussion

3.1. AgNPs/PDOP/AAOs

In the first part, we prepared PDOP-coated nanopores using dopamine as a monomer and AAO membranes as the template material (Scheme 1a). X-ray photoelectron spectroscopy (XPS) was used to confirm the PDOP coating and AgNP formations on the AAO surface. Fig. 1 shows the XPS spectra of pristine AAO, PDOP-coated AAO and AgNPs impregnated PDOP/AAO surfaces. It can be seen in the figure that the binding energies of Al 2p, Al 2s and O 1s peaks are approximately 77.6, 122.4 and 534.4 eV, respectively, corresponding to characteristic regions of an anodic alumina membrane (Fig. 1a). A weak C1s peak at 292.8 eV was due to minor hydrocarbon contamination. The PDOP-coated AAO surfaces also exhibited C (1s: 287.2 eV) and N (1s: 401.6 eV) peaks in addition to characteristic AAO peaks (Fig. 1b). After the formation of AgNPs on PDOP layers, XPS spectra showed that there were strong $Ag3d_5$ peaks at 370.4 eV ($3d_{1/2}$) and 376.8 eV ($3d_{3/2}$), confirming the formation of AgNPs (Fig. 1c). Prepared silver nanoparticles on the PDOP layer were crystalline and displayed four distinct peaks at the 2θ values of 38.1°, 44.3°, 64.5° and 77.6°, corresponding to the (1 1 1), (2 0 0), (2 2 0), and (3 1 1) crystalline planes of silver.

The formation of AgNPs on the PDOP-coated AAO was also confirmed through SEM (Fig. 2a and b). When compared with the pristine AAO membrane (Fig. S1), AgNPs were successfully formed on the top and sides of the PDOP-coated porous AAO. In addition, the nanoparticle density for 24 h polymerization was significantly higher than for 3 h (Fig. S1B). Moreover, the reductive capacity of the PDOP layer was apparently sufficient to eliminate the reducing agent in the metal salt solution.

The catalytic activities of the AgNPs/PDOP/AAO substrates were examined in the reduction of o-NA using sodium borohydride as the stoichiometric reducing agent. This activity was critical because such aromatic nitro compounds are one of the most refractory pollutants resulting from the production of pesticides, herbicides, insecticides, and synthetic dyes in industrial wastewaters [18,19]. The United States Environmental Protection Agency (USEPA) also lists nitrophenols among the top 114 organic pollutants. Therefore, this model reaction not only allows investigation of catalytic properties, but it is also interesting from the point of view of pollution abatement.

As a control experiment, the catalytic activity of individual AgNPs (approximately 18 nm) was first examined. The peak at 410 nm gradually decreased with time, a behavior that was attributed to the reduction of yellow-colored o-NA in solution. Complete conversion was observed in 20 min (Fig. S2a). Notice that the catalysis reaction in the absence of AgNPs was quite slow and that only 3% of the o-NA molecules were converted to BDA after 24 h (Fig. S2b). Next, the catalytic efficiencies of modified AAO membranes were tested. Fig. 3a–c shows the UV–vis spectra for the reduction of o-NA using modified-AAO membranes of various pore sizes. After immersing the AgNPs/PDOP/AAOs, the peak height at 410 nm rapidly decreased for all situations. The catalytic conversions were completed in 20 min for the AAO with a 200 nm pore size, 25 min for the 100 nm pore size and 30 min for the 20 nm pore size.

These catalytic differences were due to various reasons. First and foremost, formations and densities of AgNPs in the pore walls were different. In the case of this report, the driving force for the nanoparticle formation was redox active catechol and amine groups in the PDOP structure. To understand this effect, we tested the effect of PDOP thickness on the formation of AgNPs in AAO membranes having the same pore size. We found that the o-NA conversion was complete in 20 min for the AgNPs formed on PDOP film with a 37.4 nm thickness, while approximately 57.4% of the o-NA remained for the 6.31 nm thick polymer film (Fig. S3a).

Another important effect for the difference in catalysis was the nanoporous structure. The surface area of the AAO membranes was calculated using $\pi r^2 \times D \times P$, where r is pore radius, D is film thickness, and P is pore density (all geometrical dimensions estimated from the SEM observations). We found that the surface area of membranes was 7.81 m^2 for the 20 nm AAO, 2.01 m^2 for the 100 nm AAO and 1.13 m^2 for the 200 nm AAO. Although surface areas decreased with increasing pore size, catalysis efficiency was improved, and the reduction reaction was completed in a shorter time. This phenomenon could be attributed to a lack of diffusion of o-NA molecules or insufficient polymerization of dopamine in the pores to reduce the silver salts. We also tested this surface area phenomenon using planar PDOP-coated silicon surfaces (1 cm × 1 cm).

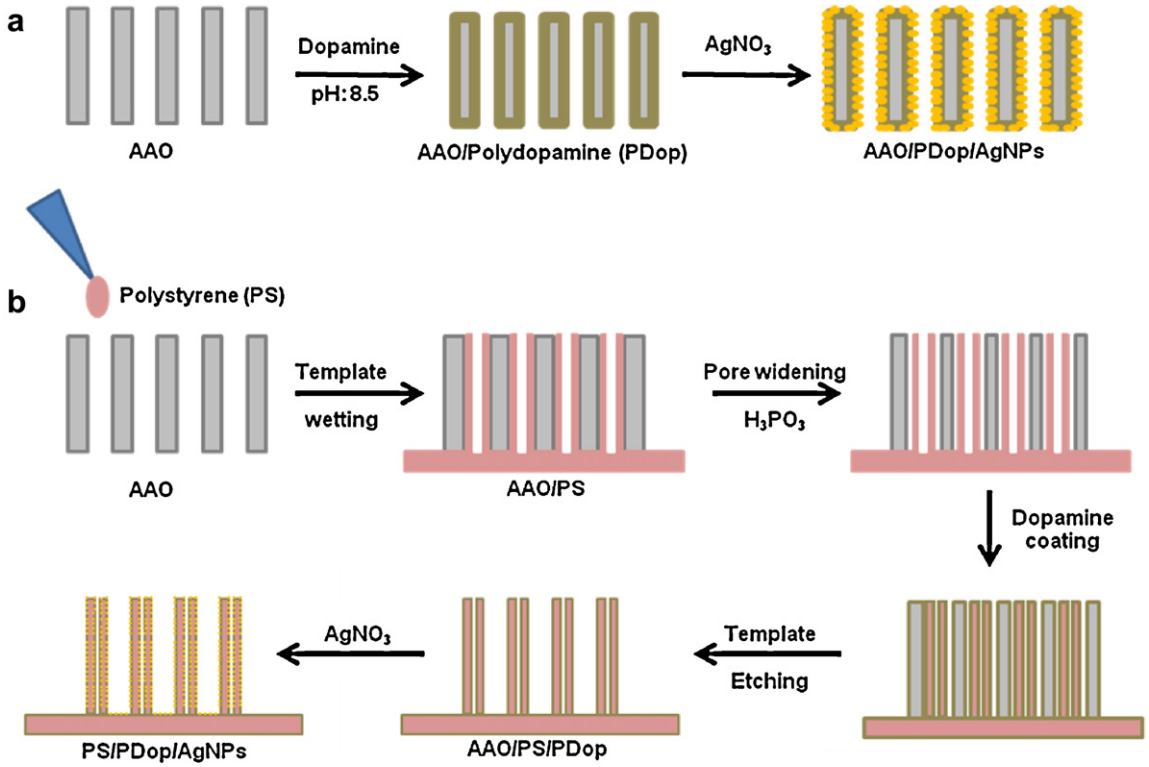

Scheme 1. Preparation of AgNPs/PDOP/AAO (a) and AgNPs/PDOP/PS nanotube (b) platforms.

The o-NA conversion was complete in 20 min for an AAO membrane having a 200 nm pore size, while 58.8% remained in the same time interval for silicon surfaces (PDOP thickness was identical for both situations) (Fig. S4).

The kinetics of the reduction reaction was also determined in the presence of the title materials. Our reaction conditions maintained first order kinetics with respect to o-NA ($\ln[C] = kt + \ln[C_0]$). The $\ln(C)$ vs. time (T) plot showed a linear correlation for o-NA

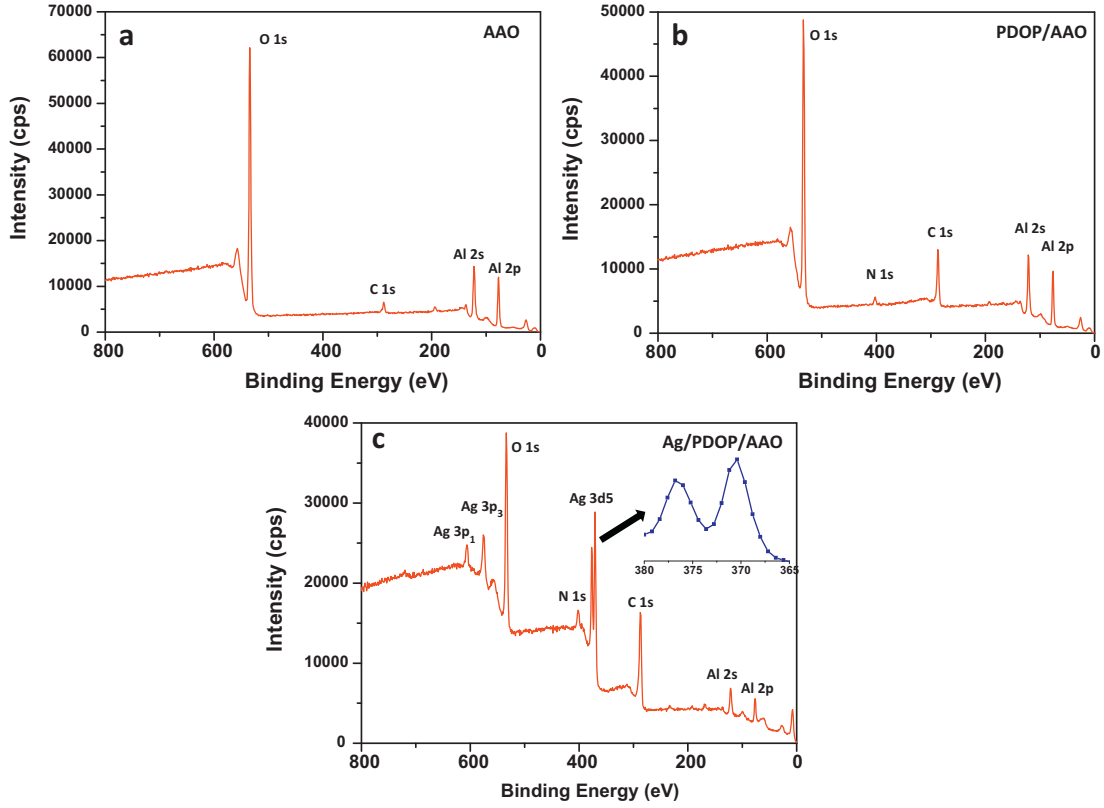

Fig. 1. XPS spectra of pristine AAO (a), PDOP-coated AAO (b), and AgNPs/PDOP/AAO (c).

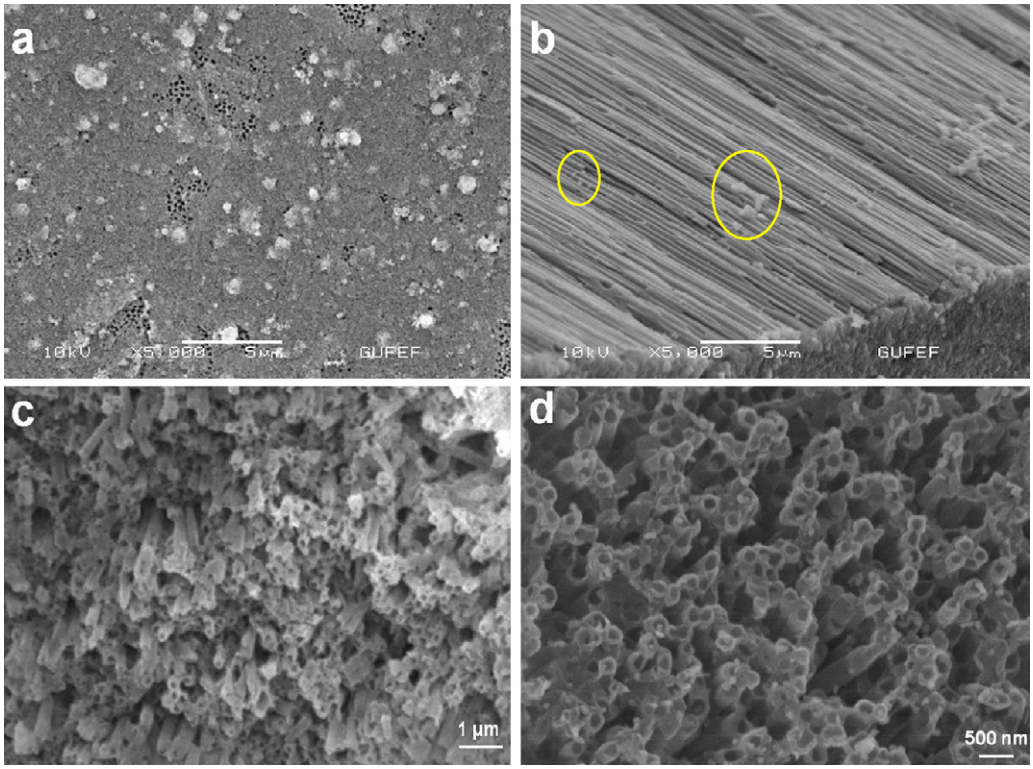

Fig. 2. SEM images of AgNP formations: (a) on the top and (b) side walls of PDOP/AAO with a 200 nm pore size, and (c) before and (d) after AgNP formation on the PDOP/PS nanotubes.

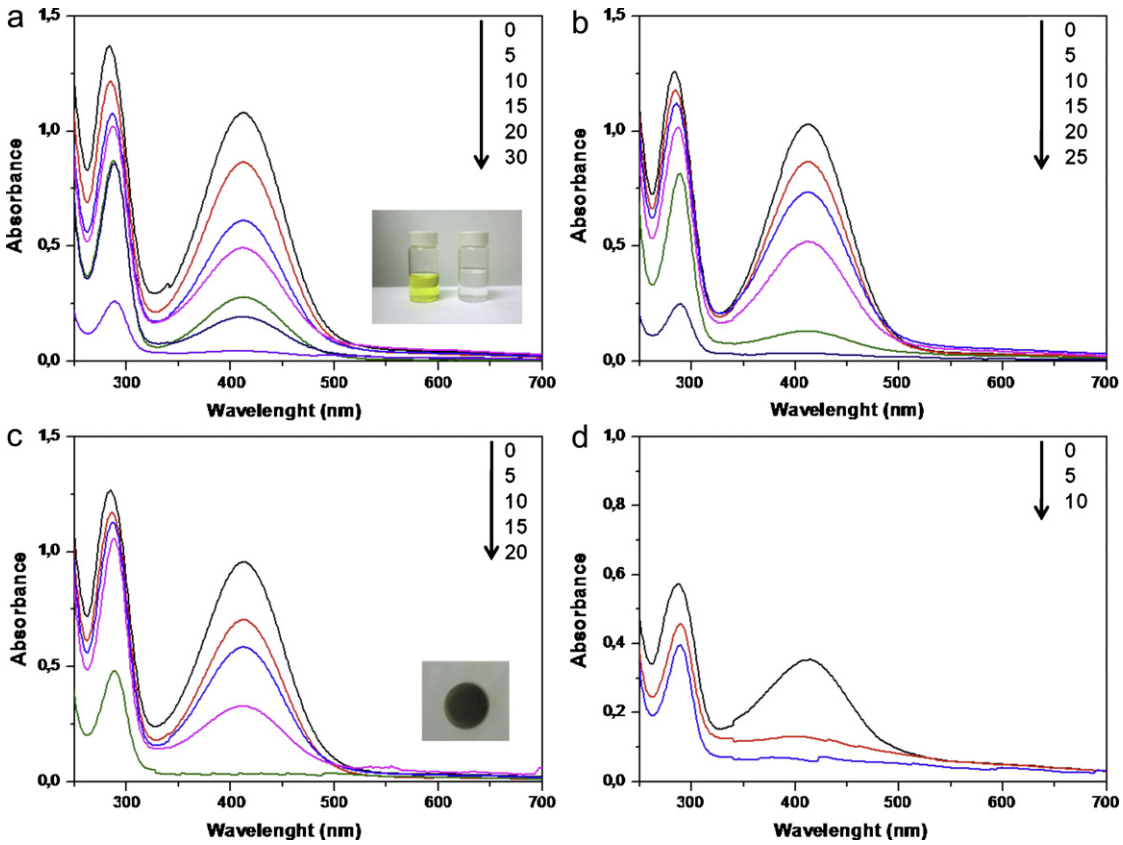

Fig. 3. UV–vis spectra of aqueous solutions of o-NA and $NaBH_4$ in the presence of (a) AgNPs/PDOP/AAO (20 nm) (photos of the o-NA solution before and after reduction in the inset), (b) AgNPs/PDOP/AAO (100 nm), (c) AgNPs/PDOP/AAO (200 nm) (a photo of the AgNPs/PDOP/AAO in the inset), and (d) AgNPs/PDOP/PS nanotubes.

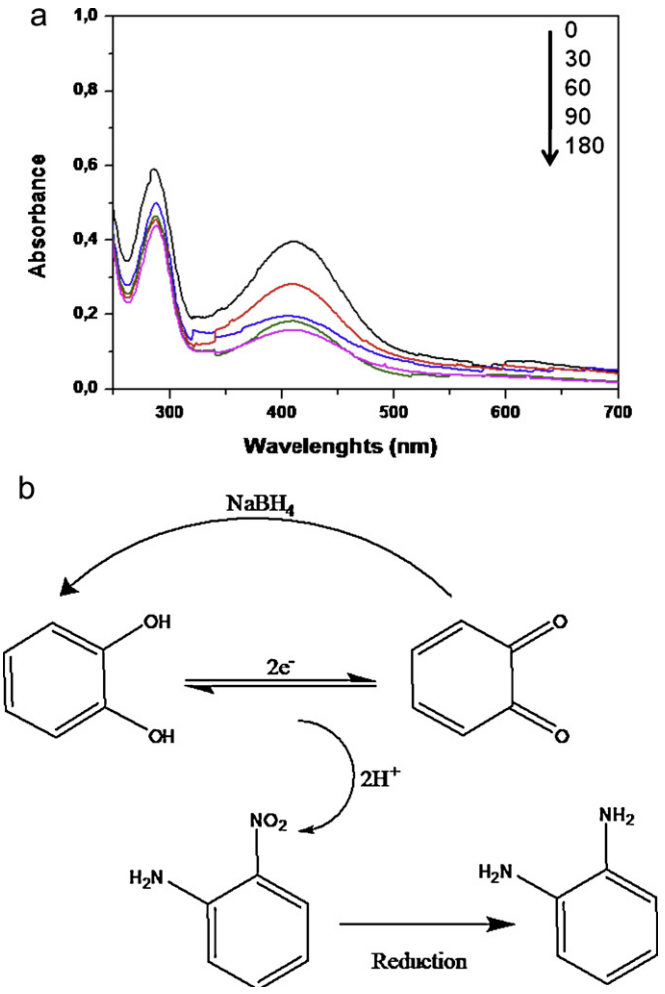

Fig. 4. UV–vis spectra of o-NA reduction by PDOP-coated AAO without AgNPs (a) and a possible mechanism for reduction (b).

reduction, where C and C_0, the concentrations of o-NA initially and at time t, respectively, were calculated based on absorbance at 410 nm by establishing a standard working curve (Fig. S5a). The rate constant (k) for the individual AgNPs and AgNPs/PDOP/AAO-200 nm were estimated to be 6.1×10^{-2} min^{-1} and 7.9×10^{-2} min^{-1}, respectively (Fig. S5b and c).

3.2. AgNPs/PDOP/PS nanotubes

To increase the PDOP-coated surface area and improve handling, we prepared polystyrene (PS) nanotubes with 200 nm pores prepared using a template-based wetting approach (Scheme 1b) [20–22]. Fig. 2c shows the well-aligned, high aspect ratio, and closely packed PS nanotubes with diameters having a narrow diameter distribution around 200 nm (±13 nm). After 24 h of PDOP polymerization, AgNPs were formed spontaneously on the inner and outer walls of the polymeric nanotubes (Fig. 2d). The catalytic properties of the AgNPs/PDOP/PS nanotubes were examined as mentioned above. We observed that the catalytic conversion was completed after 10 min (Fig. 3d). As we expected, when the PDOP-coated surface area was increased during the pore-widening process, AgNPs formed more densely on the inner and outer walls of the PS nanotubes. As a result, the reduction of o-NA was accelerated. In the literature, there are several works about using supported AgNPs for catalytic reduction of nitro compound [23–29]. In order to compare our results with other reported results, we have made a table. When all overall conversion times which were obtained using different substrate concentrations were considered, AgNPs/PDOP/PS was showed quite fast conversion efficiency (Table 1).

Table 1
A comparison of catalytic activities of supported AgNP systems.

Support material	Substrate concentration	Overall conversion time
Poly(vinylpyrrolidone) modified glass [23]	2.0×10^{-4} M	27 min
Mesoporous silicate [24]	9.0×10^{-5} M	17 min
Al_2O_3 [25]	4.0×10^{-3} M	22 min
Poly(vinyl alcohol) hydrogel [26]	1.2×10^{-4} M	10 min
DNA [27]	1.0×10^{-4} M	6 min
Poly(acrylonitrile-co-vinyl acetate) microsphere [28]	3.0×10^{-6} M	50 min
Calcium Alginate [29]	1.0×10^{-4} M	8 min
This work (for PDOP/PS nanotubes)	3.4×10^{-3} M	10 min
This work (for PDOP/AAO 200 nm)	3.4×10^{-3} M	20 min

Furthermore, the catalytic operational stability of AgNPs/PDOP/PS was evaluated. In all cases, substrates were first removed from the catalysis medium and washed with deionized water several times, then reintroduced into a fresh solution. The catalysts were found to retain about 78% of their relative activity after 5 rounds of recycle.

3.3. PDOP coating without AgNPs

Interestingly, the PDOP layers were found to be enhanced o-NA reduction in nanopores. To understand this effect, we prepared PDOP-coated AAO surfaces without AgNPs employed them in catalysis. Although, the catalytic reaction was slow, approximately 56.2% of the o-NA molecules were converted to BDA in 180 min (Fig. 4a). It is known that catechol groups are redox active molecules and that they can be transformed to 1,2-benzoquinone in the presence of an oxidant (in our case, o-NA) via a reversible two-electron, two-proton oxidation [30]. In this reaction, o-NA molecules are reduced to BDA, and catechol groups are oxidized to 1,2-benzoquinone. While this reaction proceeded, $NaBH_4$ in the catalysis medium also acted as a reducing agent to regenerate catechol from 1,2-benzoquinone (Fig. 4b), driving the catalytic reduction of o-NA. An electron transfer process between the PDOP layer and the o-NA might have been another important reason for the observed catalytic activity. In this reduction process, o-NA molecules first interacted with the PDOP layer, and electron transfer occurred from the BH_4^- and/or PDOP to the o-NA [31]. However, modeling and more detailed experiments are still needed to better understand this phenomenon.

4. Conclusions

In summary, we demonstrated the activity of supported-metal catalysts based on a bio-inspired polymer coating with electroless plating of silver nanoparticles onto nanomaterials for the catalytic reduction of aromatic nitro compounds. Our results indicated that the reduction reaction was fastest in the presence of AgNPs/PDOP/PS. We also found that the PDOP coating alone had the ability to reduce o-NA to BDA. We believe that a PDOP coating combined with an electroless plating approach provides greater flexibility in the selection of support materials and nanoparticles for a variety of catalytic reactions.

Acknowledgment

The authors wish to thank Dr. Hamdi Ozkan for a number of useful discussions. This work was supported by the Turkish Ministry of Industry and Trade (Project No. 00367.STZ.2009-1). G.D. gratefully acknowledges Gazi University for financial support (Project No. 05/2010-83 and 05/2010-17). E.P. was also supported by the Turkish Academy of Science as a full member.

Appendix A. Supplementary data

Supplementary data associated with this article can be found, in the online version, at doi:10.1016/j.molcata.2011.09.017.

References

[1] M. Madhavan, C.W. Jones, M. Weck, Acc. Chem. Res. 41 (2008) 1153.
[2] N.E. Leadbeater, M. Marco, Chem. Rev. 102 (2002) 3217.
[3] S. Rendler, D.W.C. MacMillan, J. Am. Chem. Soc. 132 (2010) 5027.
[4] S. Ogasawara, S. Kato, J. Am. Chem. Soc. 132 (2010) 4608.
[5] A. Ahosseini, W. Ren, A.M. Scurto, Ind. Eng. Chem. Res. 48 (2009) 4254.
[6] F. Jutz, J.M. Andanson, A. Baiker, Org. Process Res. Dev. 12 (2008) 950.
[7] P. Pelphrey, J. Hansen, H.M.L. Davies, Chem. Sci. 1 (2010) 254.
[8] G. Stavber, M. Zuban, S. Stavber, Tetrahedron Lett. 47 (2006) 8463.
[9] M.A. Brookshier, C.C. Chusuei, D.W. Goodman, Langmuir 15 (1999) 2043.
[10] L. Sun, R.M. Crooks, Langmuir 18 (2002) 8231.
[11] S. Jana, S. Pande, S. Panigrahi, S. Praharaj, S. Basu, A. Pal, T. Pal, Langmuir 22 (2006) 7091.
[12] A. Fukuoka, N. Higashimoto, Y. Sakamoto, S. Inagaki, Y. Fukushima, M. Ichikawa, Top. Catal. 18 (2002) 73.
[13] H. Lee, S.M. Dellatore, W.M. Miller, P.B. Messersmith, Science 318 (2007) 426.
[14] S.M. Kang, I. You, W.K. Cho, H.K. Shon, T.G. Lee, I.S. Choi, J.M. Karp, H. Lee, Angew. Chem. Int. Ed. 49 (2010) 9401.
[15] J. Ryu, S.H. Ku, H. Lee, C.P. Park, Adv. Funct. Mater. 20 (2010) 2132.
[16] H. Lee, J. Rho, P.B. Messersmith, Adv. Mater. 21 (2009) 431.
[17] S.H. Ku, J. Ryu, S.K. Hong, H. Lee, C.P. Park, Biomaterials 31 (2010) 2535.
[18] T. Vincent, E. Guibal, Langmuir 19 (2003) 8475.
[19] S. Panigrahi, B. Basu, S. Praharaj, S. Pande, S. Jana, A. Pal, S.K. Ghosh, T. Pal, J. Phys. Chem. C 11 (2007) 4596.
[20] M. Steinhard, J.H. Wendorff, A. Greiner, R.B. Wehrspohn, K. Nielsch, J. Schiling, J. Choi, U. Gosele, Science 296 (2002) 1997.
[21] G. Demirel, N. Malvadkar, M.C. Demirel, Thin Solid Films 518 (2010) 4252.
[22] G.O. Ince, G. Demirel, K.K. Gleason, M.C. Demirel, Soft Matter. 6 (2010) 1635.
[23] Q. Zhou, G. Qian, Y. Li, G. Zhao, Y. Chao, J. Zheng, Thin Solid Films 516 (2008) 953.
[24] B. Naik, S. Hazra, V.S. Prasad, N.N. Ghosh, Catal. Commun. 12 (2011) 1104.
[25] J.N. Solanki, Z. Venkata, P. Murthy, Ind. Eng. Chem. Res. 50 (2011) 7338.
[26] E. Hariprasad, T.P. Radhakrishnan, Chem-Eur. J. 16 (2010) 14378.
[27] L. Zheng, R. Zhang, Y. Ni, Q. Du, X. Wang, J. Zhang, W. Li, Catal. Lett. 139 (2010) 145.
[28] H. Xiao, Y. Xia, Polym. Eng. Sci. 50 (2010) 1767.
[29] S. Saha, A. Pal, S. Kundu, S. Basu, T. Pal, Langmuir 26 (2010) 2885.
[30] D.N. Rao, R.P. Mason, J. Biol. Chem. 262 (1987) 11731.
[31] J. Huang, L. Zhang, B. Chen, N. Ji, F. Chen, Y. Zhang, Z. Zhang, Nanoscale 2 (2010) 2733.